SCIENTIFIC REPORTS

OPEN

SUBJECT AREAS:
SKIN MODELS
ANIMAL DISEASE MODELS

Received
16 December 2013

Accepted
5 February 2014

Published
25 February 2014

Correspondence and requests for materials should be addressed to A.K. (casuaki@hama-med.ac.jp)

Potential application of in vivo imaging of impaired lymphatic duct to evaluate the severity of pressure ulcer in mouse model

Akira Kasuya, Jun-ichi Sakabe & Yoshiki Tokura

Department of Dermatology, Hamamatsu University School of Medicine, Japan.

Ischemia-reperfusion (IR) injury is a cause of pressure ulcer. However, a mechanism underlying the IR injury-induced lymphatic vessel damage remains unclear. We investigated the alterations of structure and function of lymphatic ducts in a mouse cutaneous IR model. And we suggested a new method for evaluating the severity of pressure ulcer. Immunohistochemistry showed that lymphatic ducts were totally vanished by IR injury, while blood vessels were relatively preserved. The production of harmful reactive oxygen species (ROS) was increased in injured tissue. In vitro study showed a high vulnerability of lymphatic endothelial cells to ROS. Then we evaluated the impaired lymphatic drainage using an *in vivo* imaging system for intradermally injected indocyanine green (ICG). The dysfunction of ICG drainage positively correlated with the severity of subsequent cutaneous changes. Quantification of the lymphatic duct dysfunction by this imaging system could be a useful strategy to estimate the severity of pressure ulcer.

Pressure ulcers are caused by compressions of the soft tissue, when a patient remains in a single decubitus position for a period. The bedridden old persons and critically ill patients tend to be affected. It is currently a large problem in the aging society. The mechanism of pressure ulcer is traditionally considered as compression induced ischemia, while other etiologies such as tissue deformity[1] and ischemia-reperfusion (IR) injury[2,3] have been reported recently.

IR injury consists of the ischemia by vascular occlusion and the subsequent disorder by reperfusion. In general, reperfusion of ischemic tissues yields excessive inflammation, as represented by clinical severe edema, histological infiltrate of inflammatory cells, and production of proinflammatory cytokines including tumor necrosis factor (TNF)-α, interleukin (IL)-1β and IL-6. Oxidative stress mediated by reactive oxygen species (ROS) is also involved in IR injuries of internal organs as observed in cerebral infarction and myocardial infarction[4–6]. ROS are chemically reactive molecules containing superoxide anions, hydroxyl radicals, and hydrogen peroxide. The infiltrating inflammatory cell and the damaged tissue itself produce ROS, which cause harmful oxidative stress and give rise to severe damage toward the tissues compared to simple ischemia. ROS inflict damages to DNA, cause peroxidation of lipid and proteins, and inactivate important enzymes[7]. However, in cutaneous IR injury, there has been no extensive study on the oxidative stress in the skin.

The mechanism of the damage to blood vessels has been reported in IR injury. The pathogenesis of IR injury begins with a hypoxic insult to the vascular endothelial cells, which promotes leukocyte-endothelial cell adhesion and neutrophil migration through the endothelial barrier[8,9]. As a result, microvascular permeability causes extravascular fluid leakage and edema formation[10]. Because of the damage of vascular endothelium, endothelium-dependent relaxation is also decreased. However no study has been performed regarding the damage to lymphatic ducts.

We hypothesized that a breakdown of the function of lymphatic ducts also might play important role in causing stagnant drainage of tissue fluid, leading to a severe damage. Therefore quantification of lymphatic damage might provide a new strategy for evaluating the severity of pressure ulcer. To test this hypothesis, we investigated the damage of lymphatic ducts in cutaneous IR injury by using an already established mouse model[3,11]. Results suggest that the lymphatic duct is disrupted more severely than the blood vessel is. Next, by in vitro study, we compared lymphatic and blood vasculatures in the vulnerability to anoxia and/or oxidative stress using cultured lymphatic endothelial cells (LEC) and vascular endothelial cells (VEC). Finally, we evaluated the function of lymphatic ducts using indocyanine green (ICG) as a fluorescence-emitting source.

Results

Disappearance of lymphatic ducts in IR injury. In normal Balb/c mouse skin, LYVE-1$^+$ lymphatic ducts (green) and CD31$^+$ blood vessels (red) were detected by immunofluorescence staining (Figure 1B). To create skin ischemia, the dorsal skin of Balb/c mice was gently pulled up and placed between two cylinders of magnets (12 mm in diameter), producing a compressive pressure of 50 mmHg between the two magnets (Figure 1A). In the skin treated with 16 hr-ischemia and subsequent reperfusion, lymphatic ducts, as assessed by LYVE-1 immunoreactivity, disappeared at 8 hrs after reperfusion, while CD31$^+$ blood vessels retained (Figure 1C). At this time point, the lymphatic and blood vasculatures in the marginal zone were not damaged (Figure 1F). On day 8, the IR injured tissue necrotized, and no lymphatic duct and no blood vessel was observed (Figure 1D). The lymphatic vessels were regenerated in the granulation tissue formed in the marginal zone (Figure 1G). The ulcer was completely healed on day 14 with regenerated epidermis (Figure 1E). The immunoreactivities reappeared in lymphatics (green) and blood vasculatures (red) in both IR area (Figure 1E).

The luminal areas and numbers of blood vessels (Figure 1I) and lymphatic ducts (Figure 1J) were measured in the IR area and marginal zone of the 8-hr reperfusion skin. Compared to the marginal zone, the IR area showed reduced number and luminal area of lymphatic ducts, but blood vessels were not vanished (Figure 1I, 1J).

Oxidative stress induced by IR injury. In the 16-hr IR injured tissue at 8 hrs after reperfusion, neutrophils infiltrated in the dermis and subcutaneous fat (Figure 2A). By immunofluorescence staining, there were a large number of cells bearing 8-hydroxy-2′-deoxyguanosine (8OHdG; red), a common stress marker of DNA damage (Figure 2B). Normal skin specimen exhibited no neutrophils and no staining of 8OHdG (Figure 2C, 2D). The amount of H_2O_2 was measured in the tissue (Figure 2E) and serum (Figure 2F). Their levels were significantly increased in both samples, indicating that ROS were produced by IR injury and created 8OHdG in the DNA of tissue-resident cells.

High vulnerability of lymphatic endothelial cells to oxidative stress. LEC and VEC were cultured with H_2O_2 at varying concentrations. Viability assay showed that the addition of H_2O_2 decreased the viability of LEC more profoundly than that of VEC (Figure 3A, 3B), indicating susceptibility of LEC to oxidative stress. After addition of H_2O_2 to the culture, ROS accumulated intracellularly at a significantly higher level in LEC than in VEC (Figure 3C). The reoxygenation after 3-hr culture in an anoxic condition brought about intracellular accumulation of ROS in LEC, but not in VEC (Figure 3D). The activity of SOD, which is a crucial antioxidant in live cells, was lower in LEC than in VEC (Figure 3E). $CoCl_2$, which induces a chemical ischemia, decreased the viability levels of LEC and VEC to comparable degrees (Figure 4A, 4B). Similarly, simple anoxia

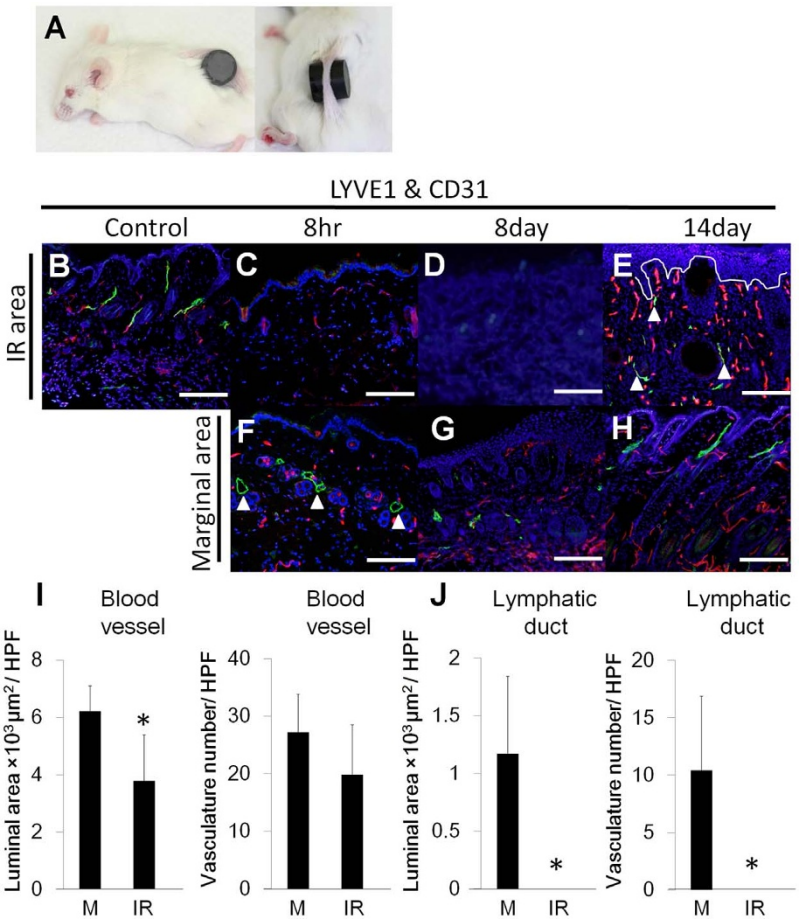

Figure 1 | Immunohistochemistry for lymphatic ducts and blood vessels in IR injury with 16-hr ischemia. (A) IR injury model. (B) Lymphatic ducts (LYVE-1; green fluorescence) and blood vessels (CD31; red fluorescence) in normal control without IR. Chronological changes at IR area (C–E) and marginal area (F–H). Scale bar, 50 μm. IR area is the place that is clamped by magnets. Marginal area is the area around the IR area. Eight hrs after reperfusion, lymphatic ducts totally disappear (C), while dilated lymphatic ducts (▶; arrow head) are observed in the marginal area (F). On Day 14 when the ulcer was healed, lymphatic ducts (▶, arrowhead) are regenerated in IR area (E). The white line is the border of the regenerated epidermis and dermis (E). Vertical bars represent the means ± SEM of the luminal area and vasculature number of blood vessels (I) and lymphatic ducts (J) at 8 hrs after reperfusion. Significant differences between sample means are indicated, *$P < 0.05$ versus marginal area. $n = 5$, in each group.

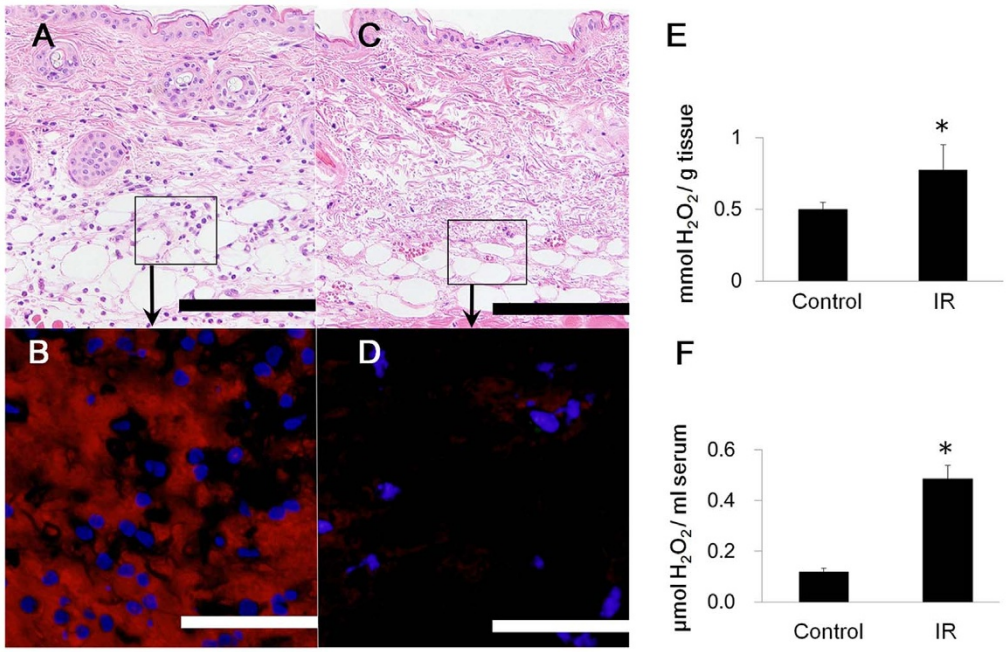

Figure 2 | Oxidative stress in IR injury. (A) Representative histological tissue sections (hematoxylin and eosin staining) shows massive infiltration of neutrophils in IR-injured skin of 16-hr ischemia at 8 hrs after reperfusion. Scale bar, 20 μm. (B) Immunohistochemistry for 8OHdG (red fluorescence). Scale bar, 10 μm. The red fluorescence shows the 8OHdG, suggesting the oxidative stress around the infiltrating neutrophils. (C), (D) Control images of normal cutaneous tissue (c; scale bar, 20 μm, d; scale bar, 10 μm). (E), (F) ROS in serum and IR injured tissue at 8 hrs after reperfusion. All values represent the mean ± SEM from more than five mice. Significant differences between the means are indicated, *P < 0.05 versus control. n = 4, in each group.

induced by a deoxidant decreased the viability levels of LEC and VEC comparably (Figure 4C). Thus, LEC are fragile to oxidative stress but not to simple anoxia as compared to VEC.

Dysfunction of lymphatic ducts induced by IR injury. ICG was injected into the dermis between two magnet-pressed areas, and images of the lower body of mice were taken by *in vivo* imaging system. A prompt increase of fluorescence at the injected site was detected (Figure 5A). While the fluorescence rapidly decreased in control mice, 16-hr IR apparently delayed the clearance, indicating the dysfunction of lymphatic duct drainage of ICG. In a comparison among 4-hr to 16-hr IR, longer ischemia times caused a more

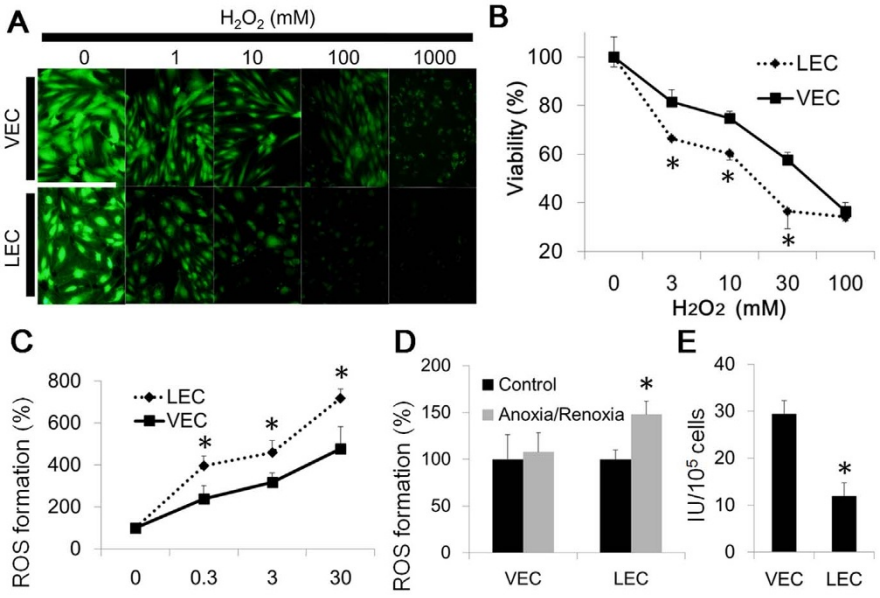

Figure 3 | Vulnerability of LEC and VEC to oxidative stress. (A), (B) Viability assay for oxidative stress induced by H_2O_2. Representative fluorescence image (A, scale bar, 10 μm) and the intensity of fluorescence (B). Viability of LEC decreased more severely than VEC. (C) Intracellular ROS produced by H_2O_2 is shown. ROS of LEC increased more severely than VEC. (D) Intracellular ROS accumulation induced by anoxia stress followed by reoxygenation. ROS accumulated in LEC more markedly than VEC. (E) Intracellular SOD activity, which is lower in LEC than VEC. All values represent the mean ± SEM from more than five wells. Significant differences between the means are indicated, *P < 0.05 versus VEC in (B), (C), (E) and versus control in (D). n = 4, in each group.

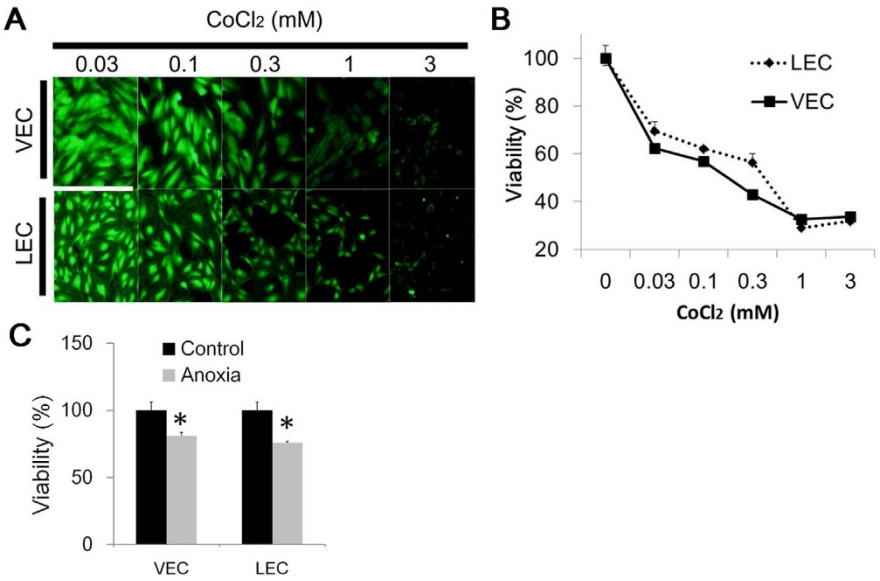

Figure 4 | Vulnerability of LEC and VEC to anoxia stress. (A), (B) Viability assay for chemical ischemia induced by $CoCl_2$. Fluorescence image (A) and the intensity of fluorescence (B). Viability of LEC and VEC decreased to the comparable levels. All values represent the mean ± SEM from more than five wells. Significant differences between the means are indicated, *P < 0.05 versus control in (C). n = 4, in each group.

profound delay of ICG clearance (Figure 5B). In a group of 'IR-16 hr (injection of ICG on day 14)', 16-hr IR was implemented. In this group, ICG was injected to IR area only after the ulcer was healed completely on day 14. The intensity of fluorescence dropped on day 15, indicating the restoration of the drainage function of lymphatic ducts (Figure 5B, from day14 to day 16).

We also observed the skin manifestation in mice receiving IR of different ischemia times (4, 8, 12, and 16 hrs). ICG was injected just before the reperfusion. Purpura and ulcer (Figure 6A) were monitored at varying days after reperfusion. Four-hr IR induced no macroscopic change throughout monitoring period (Figure 6B). In 8-hr IR, mice exhibited a low level of purpura without ulcer. Purpura was induced by 12 hr IR in all mice without ulcer. In 16-hr IR, purpura was evoked and followed by ulcer formation in all mice.

We plotted the ischemia time and ICG fluorescence intensity at the time points of 1, 2 and 4 days after reperfusion and found that longer ischemic time resulted in larger retention of ICG (Figure 7). In particular, a linear correlation of the fluorescence intensity with the ischemia time was observed on day 4 after reperfusion (Figure 7, right). On this post-reperfusion day, 4-hr ischemia caused no symptom with the ICG fluorescence intensity of $\sim 0.5 \times 10^3$ scaled counts/sec; 8-hr and 12-hr ischemia treatments induced purpura with ~ 1.25 and 2.5×10^3 scaled counts/sec, respectively; and 16-hr ischemia caused ulcer with $\sim 3.5 \times 10^3$ scaled counts/sec.

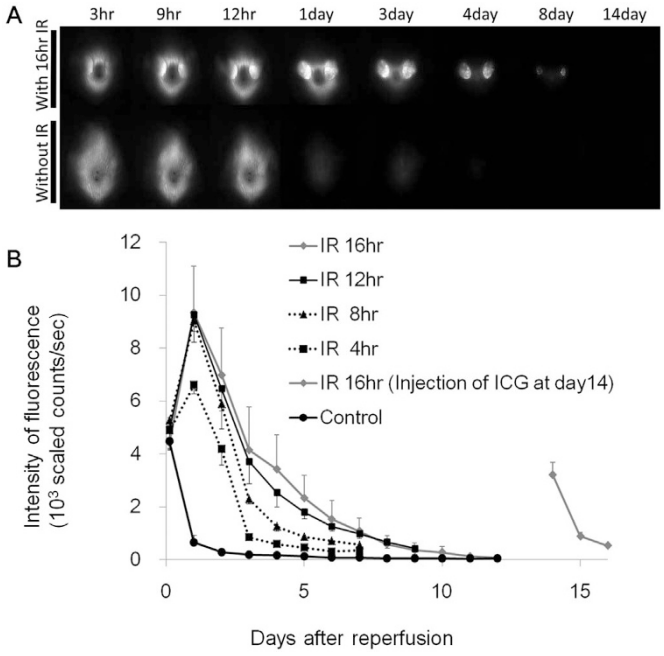

Figure 5 | Chronological change of fluorescence intensity of ICG. (A) Fluorescence image after injection of ICG with IR and without IR. (B) Quantified fluorescence intensity with various IR time. n = 10 area, in each group.

Discussion

Pressure ulcers are associated with vascular occlusion, deformity of tissues[1] and IR injury. In the mouse model for cutaneous IR injury, the macroscopic and histological changes and the inflammatory alterations evoked by reperfusion have been investigated[3,11].

In severe stages of chronic venous insufficiency, a causative of chronic ulcer, the lymphatic capillary network is destroyed, and remaining lymphatic capillary fragments have an increased permeability to dextran with a molecular weight of 150,000[12]. However, there has been no research on the lymphatic duct impairment of pressure ulcer, which potentially causes a delay of wound healing. Our assessment of LYVE-1 expression showed that cutaneous lymphatic ducts were vanished by 16-hr ischemia and subsequent 8-hr reperfusion, while blood vessels were relatively preserved. This suggests that the lymphatic duct is more vulnerable than blood vessel to cutaneous IR injury.

To assess the dysfunction of lymphatic ducts, we injected ICG into the area of IR injury. Injected ICG usually binds to lipoprotein and is absorbed by lymphatic ducts[13]. Thus, the lymphatic dysfunction can be evaluated by detecting the stagnant drainage of ICG, whose fluorescence is quantified by *in vivo* imaging system. On day 1 after injection, the non-treated control group showed complete clearance of the ICG fluorescence. However, the IR group showed a marked delay of ICG drainage, and the delay was increased in proportion to the ischemia time. At the same time point after reperfusion, the three factors, i.e. the ischemia time, ICG fluorescence intensity, and symptom severity clearly correlated with each other. Notably, the ischemia

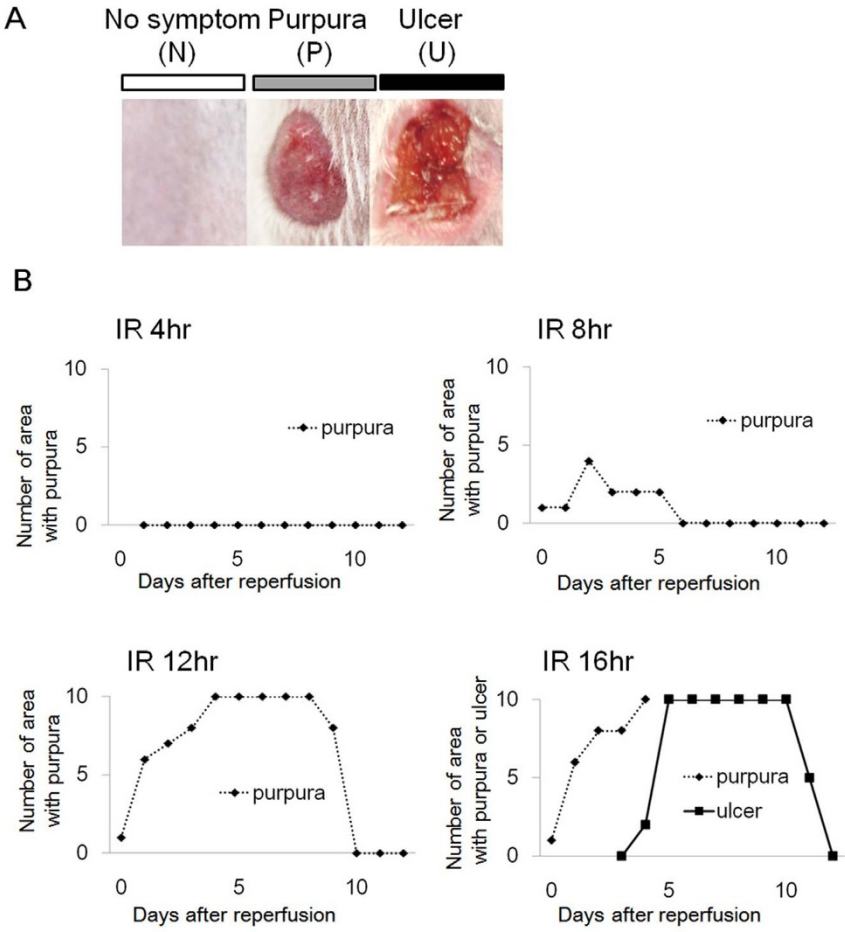

Figure 6 | Clinical symptoms induced by IR injury and the timing of its appearance. (A) Macroscopic changes (no symptom, purpura, and ulcer) induced by IR. (B) Number of IR area exhibiting purpura or ulcer (totally 10 area) at various time points after reperfusion. n = 10 area, in each group.

time and ICG fluorescence intensity showed a linear correlation at day 4 (Figure 7).

The association between the above three factors possibly allows us to predict the severity of symptoms by measuring the ICG fluorescence intensity at a certain time point after reperfusion. For example, at 4-day post-reperfusion, if the detected fluorescence intensity is less than 500 scaled counts/sec, no symptom cannot be induced. When it falls 1000 to 3000 scaled counts/sec, purpura can appear, and more than 3500 scaled counts/sec may represent ulceration. Although these values seem to be different in human clinical settings, the measurement of ICG retention could be applicable to prediction of the pressure ulcer severity.

In addition to the development of pressure ulcer, the wound healing was also associated with the lymphatic duct function and ICG fluorescence intensity. Regeneration of the damaged tissues starts on day 8 after IR from the marginal area of ulcer, where granulation tissue developed to replace the injured tissue. On day 14, lymphatic ducts and blood vessels were completely regenerated. The data from ICG injection on day 14 revealed that the ability of lymphatic ducts to drain ICG was recovered by this time point.

As to the cause of pressure ulcer, recent studies have focused mainly on compression of blood vessels and resultant ischemia. On the other hand, we found the involvement of lymphatic damage in pressure ulcer. However, it should be noted that our study showed only the fragility of lymphatic duct, the regeneration of lymphatic duct in the healed skin and some functional information on lymphatic duct fragility in the settings. Therefore, we could not estimate how severely the dysfunction of lymphatic ducts contributes to the formation of pressure ulcer.

Oxidative stress activates nuclear factor-κB (NF-κB) thereby stimulating several mediators of inflammation, which leads to vicious cycle of oxidative stress through promoted inflammatory cell infiltration[14]. Cerebral and myocardial infarctions are representative disorders mediated by oxidative stress[15]. In cerebral infarction, edaravone, a radical scavenger already clinically available[15,16], can suppress neutrophil activation and accumulation of lipid peroxidation products in mice[17]. We found that ROS were increased in serum and cutaneous tissue of IR model mice. Activated neutrophils produce superoxide anion by NADPH oxidase[17]. 8OHdG, a representative DNA alteration induced by oxidative stress[18], was observed in tissue where neutrophils were infiltrated.

We found that lymphatic ducts were more fragile to oxidative stress than blood vessels, as assessed by the viability assay (Figure 3A, 3B) and intracellular accumulation of ROS assay (Figure 3C, 3D) in a comparison between LEC and VEC. Furthermore, we used a simple model of monolayered vascular endothelial cells, which were exposed to anoxia and subsequently subjected to reoxygenation to mimic IR-induced vascular changes[19–22]. In this *in vitro* system, anoxia/reoxygenation induces the production of ROS, which induces the activation of NF-κB and the expression of endothelial surface adhesion molecules[21]. The production of ROS was higher in LEC than in VEC, and SOD activity was lower in LEC. The low activity of SOD in LEC may contribute at least partly to the vulnerability of LEC to oxidative stress.

We studied the effect of anoxia itself on LEC and VEC without reoxygenation by using two systems, the $CoCl_2$-induced chemical anoxia affecting mitochondria and attenuating cellular respiration[23], and the physical anoxia induced by oxygen absorber. These two

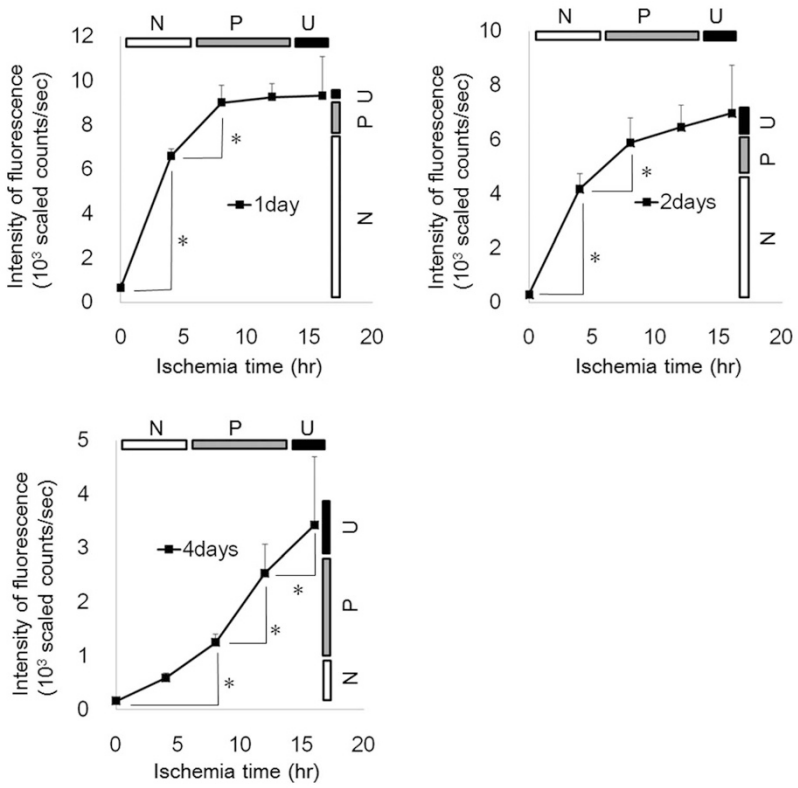

Figure 7 | Relationship between the ICG fluorescence intensity and the IR time in association with macroscopic changes at different time points after reperfusion. n = 10 area, in each group. *P < 0.05 between two groups.

systems showed that the anoxia tolerance is comparable between LEC and VEC. In the physiological condition, PO_2 in the blood vessel is considered higher than that in the lymphatic duct, as 50–40 mmHg in arterioles and 20–30 mmHg in lymphatic fluid[24,25]. Given that the higher PO_2 induces the larger oxidative stress, the high tolerance of VEC to oxidative stress may be reasonable.

The diagnosis of pressure ulcer and its severity are usually made by inspection and palpitation. Echocardiogram is effective for evaluating the deep dermis and subcutaneous tissue[26], but it is inappropriate to evaluate the early phase damage. Our study using ICG may provide a new strategy. ICG is a nontoxic substance promptly metabolized in the liver and is widely used for evaluation of lymphatic systems, including sentinel lymph node biopsy and leg lymphedema[27,28]. A portable fluorescence detection probe is now available for clinical use as an alternative of *in vivo* imaging system, and such a probe allows us to evaluate the severity of pressure ulcer in the future.

In conclusion, we showed that lymphatic duct is vulnerable to IR injury partly because of the high sensitivity to harmful ROS. And quantification of impaired lymphatic duct function provided a new method for the evaluation of pressure ulcer.

Methods

Animals. Balb/c wild-type mice were obtained from SLC inc (Tokyo, Japan). All mice were healthy, fertile, and did not display any evidence of infection or disease. Female mice (8- to 12-week-old) were used for all the experiments. All mice were housed in specific pathogen-free barrier facility and screened regularly for pathogens. Mice were individually housed in plastic cages to prevent accidental dislocation of the magnets and to prevent tampering with the resultant ulcer by other mice. All studies and procedures were approved by the Committee on Animal Experimentation of Hamamatsu University School of Medicine. And the protocol was performed in accordance with the approved guidelines.

IR cycles. The IR cycle model was previously reported[11]. Briefly, mice were anesthetized with diethyl ether and their backs were shaved and cleaned with 70% alcohol. A template was used to mark the location of the magnetic cylinders to assure a consistent placement on each mouse. The skin was gently pulled up and placed between two cylinders of ceramic magnets (Figure 1A) that had a 12-mm diameter (113 mm^2) and were 5 mm thick, with an average weight of 2.4 g and 1,000 G magnetic forces (Seiko Sangyo Co., Ichikawa, Japan). Epidermis, dermis, subcutaneous fat layer, panniculus carnosus, and subcutaneous loose connective tissue layer (hypodermis), but not muscles, were pinched with the magnetic cylinders. This process created a compressive pressure of 50 mmHg between the two magnets[2,11].

A cycle of IR was performed in each mouse. The mice were randomly assigned into each group. In the experiment of pathological estimation of lymphatic duct in IR injury, magnet was placed for 16 hrs. Mice were not immobilized, anesthetized, or otherwise treated during IR cycles. Skin tissues were harvested and used for subsequent analysis at 8 hrs, 8 days and 14 days after detachment of magnets. In the experiment of functional estimation of lymphatic ducts in IR injury, either of 0, 4, 8, 12, and 16-hr period of magnet placement was followed by observation by *in vivo* imaging system. The clinical symptoms including purpura and ulcer were checked every day until day 14 for each mouse. Some of the mice developed two circular purpura or ulcers separated by a bridge of normal skin, as reported previously[11].

The etiology of pressure ulcer is multifactorial. Our mouse model can simulate pressure, tissue compression, and ischemia-reperfusion. The limitation of this model is the failure to reflect friction and shear force. In addition, the back skin used in this study is not a body part where bones are extruded, and thus is not a predilection site for pressure ulcer.

Histological examination and immunohistochemistry. After the mice were sacrificed, wounds were harvested with a 2 mm rim of unwounded skin tissue. The wounds were cut into laterally halves, fixed in 3.5% paraformaldehyde, and embedded in paraffin. Sections were stained with hematoxylin and eosin. The other half part of the wound was embedded in O.C.T. Compound (Sakura Fine Tech Japan, Tokyo, Japan). For immunohistochemistry, fresh frozen sections were fixed with 100% methanol and treated with 3% normal chicken serum (Gibco; Life Technologies Corporation, Carlsbad, CA) for 6 minutes at room temperature. Sections were then incubated with antibodies. We used polyclonal rabbit antibody specific for CD31 (Thermo Fisher Scientific Inc., Waltham, MA), monoclonal rat antibody specific for LYVE-1 (Medical & Biological Laboratories Co., Nagoya, Japan), monoclonal mouse antibody specific for 8-OHdG (Japan Institute for the Control of Aging, Fukuroi, Japan). Alexa Fluor Secondary Detection Reagents (Life Technologies Corporation, Carlsbad, CA) was used for secondary antibody. The captured images of IHC by LYVE-1 and CD31 were analyzed by software system (Lumina Vision 1.1.1.1) for measuring the numbers and area of lymphatic duct and vascular. Data were obtained from more than five mice.

ROS measurement of serum and cutaneous tissue. For the measurement of serum and tissue reactive oxygen species (ROS), we used OxiSelect™ In Vitro ROS/RNS

Assay Kit (cellbiolabs, San Diego, CA) according to the manufacturer's protocol. Green fluorescence (excitation: 495 nm; emission:515 nm) was detected by plate reader (Synergy HT, Bio-Tek, VT).

In vivo imaging and analysis. Twenty five μl of ICG (2.5 mg/ml, Daiichi-Sankyo, Tokyo, Japan) was injected into the dermis between the two circle area where cylinder-shaped-magnets were applied. Lower-body images of mice were acquired by using *in vivo* imaging system (Maestro, CRI Inc., Santa Maria, CA; excitation: 671 to 705 nm; emission: 750 to 950 nm). The Maestro optical system uses a liquid crystal tunable filter (30 nm bandwidth; scanning wavelength range, 500 to 950 nm), a 16-bit high-resolution scientific-grade monochrome imaging sensor and Maestro 3.0.0 software for image acquisition and analysis. The imaging regions with pure autofluorescence spectra were manually selected and subtracted from the mixed fluorescence signal of the image to obtain the ICG fluorescence intensity at each imaging pixel recorded. Fluorescence intensities from the selected regions were normalized, measured, and finally, analyzed.

Cell culture. Human lymphatic endothelial cells (LEC; Lonza, Basel, Switzerland) and human vein endothelial cell (VEC; Lonza, Basel, Switzerland) were cultured in 10% fatal bovine serum containing complete endothelial cell basal medium (EBM-2; Lonza, Basel, Switzerland) supplemented with SingleQuots™ kit (Lonza, Basel, Switzerland). LEC and VEC were seeded in 10 cm culture dish, and were incubated at 37°C and 5% (v/v) CO2 and used between the first and fifth passages for all experiments. Twenty four hrs prior to the start of the assays, LEC and VEC were harvested at 70–80% confluence after digestion by 0.025% trypsin. The cells were seeded to the 96 well plate at a density of 10^4 cells/well.

Cell viability assay. Cell viability was determined by LIVE/DEAD® Viability Assay Kit (Life Technologies USA, CA) measuring the green fluorescence in live cells (ex/em ~495 nm/~515 nm) by plate reader (Synergy HT, Bio-Tek, VT).

ROS formation in live cells by hyper peroxide. To quantify the magnitude of ROS formation by hyper oxide in live cells, we used OxiSelect™ Intracellular ROS Assay Kit (Cellbiolabs, San Diego, CA) according to the manufacturer's protocol. Green fluorescence (excitation: 495 nm; emission:515 nm) was detected by plate reader (Synergy HT, Bio-Tek, VT).

Cell viability assay for oxidative stress and chemical hypoxia. Hydrogen peroxide (Wako, Tokyo, Japan) was added to the medium at the final concentration of 0, 10, 100, 1000, and 10000 μM. Cell viability was detected as previously delineated. Chemical hypoxia was induced by $CoCl_2$ (Wako, Tokyo, Japan). $CoCl_2$ was added to the medium at concentration of 0.03, 0.1, 0.3 and 1 mM. Cell viability assay was performed at 30 min after $CoCl_2$ insult.

Physical deoxygenation. Physical deoxygenation was achieved by oxygen absorber (Aneropack; Mitsubishi gas chemical company, Inc., Tokyo, Japan). Cells seeded in 96-plate were cultured for 3 hrs in an airtight chamber. For detection of ROS formation by reoxygenation, live cell ROS formation assay was followed after 3 hour exposure to atmospheric conditions. And in the experiment for analyzing anoxia tolerance, cell viability assay was performed immediately after taking cells out of chamber.

SOD activity assays. The SOD activity of LEC and VEC were measured using commercial kits (OxiSelect™ SOD Activity Assay (cellbiolabs, San Diego, CA)), according to the manufacturer's instructions.

Statistical analysis. The two-tailed unpaired Student's t-test was used to determine the level of significance of differences between the sample means, and Tukey's test was used for multiple comparisons. A p-value <0.05 was considered statistically significant.

1. Loerakker, S. *et al.* Temporal effects of mechanical loading on deformation-induced damage in skeletal muscle tissue. *Ann Biomed Eng* **38**, 2577–2587 (2010).
2. Peirce, S. M., Skalak, T. C. & Rodeheaver, G. T. Ischemia-reperfusion injury in chronic pressure ulcer formation: a skin model in the rat. *Wound Repair Regen* **8**, 68–76 (2000).
3. Saito, Y. *et al.* The loss of MCP-1 attenuates cutaneous ischemia-reperfusion injury in a mouse model of pressure ulcer. *J Invest Dermatol* **128**, 1838–1851 (2008).
4. Li, C. & Jackson, R. M. Reactive species mechanisms of cellular hypoxia-reoxygenation injury. *Am J Physiol Cell Physiol* **282**, C227–241 (2002).
5. Arda-Pirincci, P. & Bolkent, S. The role of epidermal growth factor in prevention of oxidative injury and apoptosis induced by intestinal ischemia/reperfusion in rats. *Acta Histochem* (2013).
6. McCord, J. M. Oxygen-derived free radicals in postischemic tissue injury. *N Engl J Med* **312**, 159–163 (1985).
7. Eltzschig, H. K. & Collard, C. D. Vascular ischaemia and reperfusion injury. *Br Med Bull* **70**, 71–86 (2004).
8. Eltzschig, H. K. *et al.* Endogenous adenosine produced during hypoxia attenuates neutrophil accumulation: coordination by extracellular nucleotide metabolism. *Blood* **104**, 3986–3992 (2004).
9. Luscinskas, F. W., Ma, S., Nusrat, A., Parkos, C. A. & Shaw, S. K. Leukocyte transendothelial migration: a junctional affair. *Semin Immunol* **14**, 105–113 (2002).
10. Kubes, P. Nitric oxide affects microvascular permeability in the intact and inflamed vasculature. *Microcirculation* **2**, 235–244 (1995).
11. Stadler, I., Zhang, R. Y., Oskoui, P., Whittaker, M. S. & Lanzafame, R. J. Development of a simple, noninvasive, clinically relevant model of pressure ulcers in the mouse. *J Invest Surg* **17**, 221–227 (2004).
12. Franzeck, U. K., Haselbach, P., Speiser, D. & Bollinger, A. Microangiopathy of cutaneous blood and lymphatic capillaries in chronic venous insufficiency (CVI). *Yale J Biol Med* **66**, 37–46 (1993).
13. Yoneya, S. *et al.* Binding properties of indocyanine green in human blood. *Invest Ophthalmol Vis Sci* **39**, 1286–1290 (1998).
14. Toyokuni, S. Reactive oxygen species-induced molecular damage and its application in pathology. *Pathol Int* **49**, 91–102 (1999).
15. Kikuchi, K. *et al.* The efficacy of edaravone (radicut), a free radical scavenger, for cardiovascular disease. *Int J Mol Sci* **14**, 13909–13930 (2013).
16. Kikuchi, K. *et al.* Edaravone attenuates cerebral ischemic injury by suppressing aquaporin-4. *Biochem Biophys Res Commun* **390**, 1121–1125 (2009).
17. Derochette, S. *et al.* Curcumin and resveratrol act by different ways on NADPH oxidase activity and reactive oxygen species produced by equine neutrophils. *Chem Biol Interact* (2013).
18. Kasai, H. Analysis of a form of oxidative DNA damage, 8-hydroxy-2′-deoxyguanosine, as a marker of cellular oxidative stress during carcinogenesis. *Mutat Res* **387**, 147–163 (1997).
19. Zweier, J. L., Kuppusamy, P., Thompson-Gorman, S., Klunk, D. & Lutty, G. A. Measurement and characterization of free radical generation in reoxygenated human endothelial cells. *Am J Physiol* **266**, C700–708 (1994).
20. Terada, L. S. *et al.* Generation of superoxide anion by brain endothelial cell xanthine oxidase. *J Cell Physiol* **148**, 191–196 (1991).
21. Ichikawa, H. *et al.* Molecular mechanisms of anoxia/reoxygenation-induced neutrophil adherence to cultured endothelial cells. *Circ Res* **81**, 922–931 (1997).
22. Yoshida, N. *et al.* Anoxia/reoxygenation-induced neutrophil adherence to cultured endothelial cells. *Am J Physiol* **262**, H1891–1898 (1992).
23. Fang, D. *et al.* Expression of bystin in reactive astrocytes induced by ischemia/reperfusion and chemical hypoxia in vitro. *Biochim Biophys Acta* **1782**, 658–663 (2008).
24. Wang, W. & Vadgama, P. O2 microsensors for minimally invasive tissue monitoring. *J R Soc Interface* **1**, 109–117 (2004).
25. Kerger, H., Torres Filho, I. P., Rivas, M., Winslow, R. M. & Intaglietta, M. Systemic and subcutaneous microvascular oxygen tension in conscious Syrian golden hamsters. *Am J Physiol* **268**, H802–810 (1995).
26. Aoi, N. *et al.* Ultrasound assessment of deep tissue injury in pressure ulcers: possible prediction of pressure ulcer progression. *Plast Reconstr Surg* **124**, 540–550 (2009).
27. Akita, S. *et al.* Comparison of lymphoscintigraphy and indocyanine green lymphography for the diagnosis of extremity lymphoedema. *J Plast Reconstr Aesthet Surg* **66**, 792–798 (2013).
28. Liu, Y. *et al.* Near-infrared fluorescence goggle system with complementary metal-oxide-semiconductor imaging sensor and see-through display. *J Biomed Opt* **18**, 101303 (2013).

Author contributions

A.K. involved in all the processes of planning and implementing the experiment, interpretation of data, and writing the manuscripts. J.S. involved in the process of implementing the experiment. Y.T. involved in the processes of planning the experiment, interpretation of data, and writing the manuscripts. All authors reviewed the manuscript.

Additional information

Competing financial interests: The authors declare no competing financial interests.

How to cite this article: Kasuya, A., Sakabe, J.-i. & Tokura, Y. Potential application of in vivo imaging of impaired lymphatic duct to evaluate the severity of pressure ulcer in mouse model. *Sci. Rep.* **4**, 4173; DOI:10.1038/srep04173 (2014).

This work is licensed under a Creative Commons Attribution-NonCommercial-ShareAlike 3.0 Unported license. To view a copy of this license, visit http://creativecommons.org/licenses/by-nc-sa/3.0